Semiempirical model of positron scattering and annihilation

J. Mitroy and I. A. Ivanov

Faculty of Science, Northern Territory University, Darwin, NT 0909, Australia

A two-parameter semiempirical theory of positron scattering and annihilation is developed and used to investigate the behavior of positrons interacting with the rare gases and metal vapors. The two-parameter theory is able to do a reasonable job of reproducing existing cross section and annihilation data for the rare gases. A model-potential calculation that correctly predicts the behavior of the phase shifts will also predict the energy dependence of $Z_{\text{eff}}(k)$ even if the magnitude is incorrect. Analysis of the Z_{eff} versus temperature data of Kurz *et al.* [Phys. Rev. Lett. **77**, 2929 (1996)] suggests scattering lengths of $-5.6\pm1.0a_0$, $-10.3\pm2.0a_0$, and $-56\pm15a_0$ for Ar, Kr, and Xe, respectively. Existing bound-state calculations can be used to fix the values of the semi-empirical parameters for a number of metal vapors, resulting in predicted Z_{eff} of 119, 36, and 94 for Be, Mg, and Cu at threshold. In addition to the calculations, expressions relating the threshold form of $Z_{\text{eff}}(k)$ to the complex scattering length are presented.

I. INTRODUCTION

The annihilation of positrons in atomic and molecular gases has been a topic of interest recently. There are number of interesting phenomena associated with the positron-annihilation process: among them are very large annihilation rates [1–3], high sensitivity of the rates to small changes in molecular structure [4], and rapid increase of fragmentation and annihilation rates at small temperatures [5,6]. In spite of decades of experimental study, there has been relatively little work aimed at understanding the basic mechanisms of positron annihilation and very few detailed calculations even on a system as simple as hydrogen [7].

In a recent work, Gribakin [8] developed a theoretical framework that could be used to explain the wide range of phenomena associated with positron annihilation on molecules. He postulated that there were two different mechanisms for positron annihilation, these were (i) direct annihilation and (ii) resonant annihilation. Direct annihilation describes the annihilation of the positron with the target electrons and the direct-annihilation rate was strongly correlated with the size of the elastic cross section. Resonant annihilation was mainly important for large molecules with closely spaced vibrational levels. In resonant annihilation, the positron is trapped in a Feshbach resonance associated with a vibrationally excited state. The resonant-annihilation process was suggested to be the mechanism responsible for the large annihilation rates seen for some molecules [6,8]. The work of Gribakin is based on the earlier works of Dzuba *et al.* [9,10] that did much to elucidate the mechanisms important in the positron-annihilation process. For example, the large values of Z_{eff} for the rare gases were interpreted as arising from a virtual state close to threshold. Explicit calculations of positron annihilation for complex molecules have also been reported [11–13]. The Schwinger variational calculation upon C_2H_2 by Lima and co-workers gave a very large threshold Z_{eff}, which they attributed to a zero-energy resonance or virtual state [11].

In this paper, a two-parameter theory of positron scattering and annihilation is developed to explore the underlying mechanisms for positron annihilation. Since the parameters are adjustable it is possible to explore the relationship between the elastic cross section and annihilation cross section in detail. In particular, it is seen that a realistic model-potential calculation that correctly mimics the correct phase shifts will in all likelihood correctly predict the energy dependence of the annihilation factor $Z_{\text{eff}}(k)$.

II. DETAILS OF THE MODEL

The interaction between a positron and an atom is largely dominated by two opposing interactions. First, there is the Coulomb interaction between the positron and the nucleus. This results in a repulsive interaction between the positron and unperturbed atom. This static interaction between the positron and the atom is easy to compute accurately.

However, the electronic charge cloud of the atom is perturbed whenever there is a positron nearby. The polarization of the electron charge cloud leads to an attractive interaction between the positron and the atom. The polarization potential is known to have the asymptotic form (in atomic units)

$$\lim_{r\to\infty} V_{\text{pol}}(r) \approx \frac{-\alpha_d}{2r^4}, \qquad (1)$$

where α_d is the static dipole polarizability. All the complicated many-body interactions between the positron and atomic electrons can be absorbed into the polarization potential, which is very difficult to compute exactly. In this work, a one-parameter form for the polarization potential is adopted.

The effective Hamiltonian for the positron moving in the field of the atom is

$$H = -\frac{1}{2}\nabla_0^2 + V_{\text{dir}}(\mathbf{r}_0) + V_{\text{pol}}(\mathbf{r}_0). \qquad (2)$$

The repulsive direct potential, V_{dir} is computed from the Hartree-Fock wave function of the target atom. The polarization potential is given the form

$$V_{\text{pol}}(\mathbf{r}_0) = -\frac{\alpha_d[1 - \exp(-r^6/\rho^6)]}{2r^4}. \tag{3}$$

The adjustable parameter ρ is fixed by reference to some external factor, e.g., the value of the scattering length in a high-quality *ab initio* calculation or the binding energy of a positron-atom bound state. The underlying philosophy is purely semiempirical, no attempt at determining the specific form of the polarization potential by *ab initio* techniques is made. The elastic cross section computed with this ansatz is denoted σ_ρ.

A. Positron annihilation

When positrons collide with atoms, there is always the possibility of in-flight annihilation of the positron with one of the atomic electrons. The annihilation of a positron beam during collision is most usually described by the annihilation parameter Z_{eff}. The annihilation parameter is related to the spin-averaged absorption cross section $\sigma_{\text{abs}}(k)$ by the identity [14]

$$Z_{\text{eff}}(k) = \frac{k\sigma_{\text{abs}}(k)}{\pi c r_0^2}, \tag{4}$$

where r_0 is the classical electron radius and c is the speed of light. The annihilation parameter can be computed from the wave function and is defined [7,14,15]

$$Z_{\text{eff}} = N_e \int d^3\tau |\Psi(\mathbf{r}_1, \ldots, \mathbf{r}_N)\Phi(\mathbf{r}_N)|^2, \tag{5}$$

where $\Psi(\mathbf{r}_1, \ldots, \mathbf{r}_N)$ is the antisymmetrized wave function of the target atom, $\Phi(\mathbf{r}_N)$ is the positron-scattering function, and $d^3\tau$ represents an integration over all electron coordinates. Equation (5) is not completely general as the total system wave function is assumed to have the product form $\Psi(\mathbf{r}_1, \ldots, \mathbf{r}_N)\Phi(\mathbf{r}_0)$. The expression for Z_{eff} given by Eq. (5) is *spin averaged*. In the plane-wave born approximation, where the positron wave function is written as a plane wave, the annihilation parameter is equal to the number of atomic electrons, i.e., $Z_{\text{eff}} = N_e$.

In cases where the polarization potential is sufficiently strong it is possible for the positron to attach itself to the atom and form an electronically stable bound state. Such states will decay by electron-positron annihilation with an annihilation rate (for a simple product wave function) given by [16,17]

$$\Gamma = \pi r_0^2 c N_e \int d^3\tau |\Psi(\mathbf{r}_1, \ldots, \mathbf{r}_N)\Phi(\mathbf{r}_N)|^2. \tag{6}$$

The Z_{eff} and annihilation rate Γ predicted by this simple analysis are likely to be underestimates. The attractive nature of the electron-positron interaction leads to strong electron-positron correlations that increase the electron density at the position of the positron, and consequently enhances the annihilation rate. Therefore, an enhancement factor G is used to

rescale the calculated Z_{eff} by a multiplicative factor, G, i.e., values for Γ and Z_{eff} would be computed by

$$\Gamma^G = G\Gamma_{\text{model}} \tag{7}$$

and

$$Z_{\text{eff}}^G = GZ_{\text{eff}}. \tag{8}$$

The value of G is fixed by reference to a high-quality *ab initio* calculation or to experimental data. This work is concerned with low-energy scattering and under these circumstances the relative collision-momentum distribution of the annihilating electron-positron pair is not expected to change much as the positron energy changes slightly. This means that the errors in using an energy-independent enhancement factor should not be too large. A number of other authors have previously asserted that the electron-positron correlations leading to an increased annihilation rate should depend weakly on the positron energy [8,18].

There have been many investigations of positron-atom interactions in the past that have used conceptually similar Hamiltonians [9,19–25]. However, these previous calculations have largely tried to predict either the low-energy cross section or annihilation parameter by direct calculation. For example, the binding energies of the e^+-Be and e^+-Mg systems have previously been used to tune a polarization potential and thus determine the behavior of the positron-Be and positron-Mg elastic cross sections at low energies [26]. The focus of the present work is different from these earlier efforts and seeks to explore the interrelationship between the annihilation parameter and elastic cross section.

B. Defining ρ and G

The ability of the model-potential calculations to realistically describe the low-energy elastic and annihilation cross section depends crucially upon the choice of ρ and G. A variety of sources have been used to provide the reference data that was used to fix ρ and G. The values of ρ and G, and the reference data used to fix them are listed in Table I.

Different sources of information have been used for the different classes of atoms. First, high-accuracy calculations of the threshold cross section and Z_{eff} have been used for hydrogen and helium. The cross sections and annihilation parameters of Mitroy [7,30] were used for hydrogen. This data agrees with earlier variational calculations [31–34]. The cross sections and annihilation parameters for helium are taken from the variational calculations of Humberston and co-workers [35,36]. The polarized orbital (PO) calculations of the York group have been used to define ρ for the heavier rare gases, Ne, Ar, Kr, and Xe [37–39]. Although there have been a number of experiments reporting elastic cross sections for the rare gases [40–42], the degree of scatter amongst the different experiments and the fact that no data have been taken in the threshold region mean that it is best to define ρ by reference to a high quality calculation. The agreement of the PO cross sections with experiment is as good as can be expected given the variations between the different experiments [40–42]. From a theoretical perspective, the York

TABLE I. The parameters α_d, ρ, and G for a number of atoms in the central field model. The particular numerical criteria (and their source) used to fix ρ and G are specified. The annihilation rate is given in units of 10^9 s^{-1} and is the rate with electrons in the valence subshell.

Atom	$\alpha_d (a_0^3)$	$\rho(a_0)$	Source	G	Source
H	4.5	2.051	$A = -2.10$ [30]	6.03	$Z_{\text{eff}}(k=0.1)=7.52$ [7]
He	1.383 [27]	1.500	$\delta_0(k=0.1)=0.035$ [35]	2.92	$Z_{\text{eff}}(k=0.1)=3.76$ [36]
Be	38 [28]	2.686	$\varepsilon = 0.003147$ hartree [50]	10.18	$\Gamma = 0.416$ [50]
Ne	2.67 [27]	1.510	$\delta_0(k=0.1)=0.0360$ [37]	2.26	$\langle Z_{\text{eff}}\rangle_T = 5.99$ [48]
Mg	72 [29]	3.032	$\varepsilon = 0.015612$ hartree [50]	13.2	$\Gamma = 0.943$ [50]
Ar	11.1 [27]	1.710	$\delta_0(k=0.1)=0.310$ [38]	3.02	$\langle Z_{\text{eff}}\rangle_T = 33.8$ [4]
Cu	40$^{\text{a}}$	2.558	$\varepsilon = 0.005597$ hartree [51]	18.2	$\Gamma = 0.544$ [51]
Kr	16.8 [27]	1.85	$\delta_0(k=0.1)=0.496$ [39]	4.11	$\langle Z_{\text{eff}}\rangle_T = 90.1$ [4]
Xe	27.3 [27]	1.96	$\delta_0(k=0.1)=0.884$ [39]	4.56	$\langle Z_{\text{eff}}\rangle_T = 401$ [47]

$^{\text{a}}$The polarizability for Cu was derived from unpublished model-potential calculations.

group calculations are probably the best *ab initio* calculations for the heavier rare gases since they do a reasonable job of treating electron-positron correlations (the PO expansion of the scattering wave function allows for virtual target excitation with quite high angular momentum). Single-center close-coupling scattering calculations [43] and single-center configuration-interaction calculations of positronic atoms [44–46] have shown the ability to accurately describe electron-positron correlations as long as terms with sufficiently large angular momentum are included in the expansion of the wave function. Further evidence for the reliability of the PO calculations is apparent from the comparison of their computed Z_{eff} with other high-precision calculations and experiment. An accurate treatment of electron-positron correlations is needed for a correct prediction of Z_{eff}. Sequences of calculations in different models performed by Ryzhikh and Mitroy [7] for hydrogen and Dzuba *et al.* [9] for the rare gases have shown that poor descriptions of the scattering dynamics lead to very poor values of Z_{eff} with the threshold Z_{eff} being grossly underestimated. In the case of helium, the York group record $Z_{\text{eff}}=3.87a_0$ and $A=-0.575a_0$ [15] that are in good agreement with the close to exact results of $Z_{\text{eff}}=3.93a_0$ and $A \approx -0.5a_0$ [35,36]. The York group calculations predictions of Z_{eff} are also in reasonable agreement with experiment for Ne and Ar (refer to Table III where the thermally averaged Z_{eff} are compared with experiment). The polarized orbital Z_{eff} for krypton and xenon, however, are 30% and 50% smaller than the recent data of the San Diego group [4,47]. While the PO model captures the basic physics of the positron-atom collision, its does not reproduce the annihilation parameter for the two heaviest rare gases in detail. Therefore, the enhancement factors, G for the rare gases were determined by normalizing to the experimental Z_{eff} of the San Diego group first [4,47], and then to the UCL group [48,49] when San Diego data were not available. The experimental data were taken from a gas of positrons at a finite temperature and, therefore, G was defined by equating the thermally averaged Z_{eff} to experiment. The thermally averaged Z_{eff}, i.e., $\langle Z_{\text{eff}}\rangle_T$ is defined by

$$\langle Z_{\text{eff}}\rangle_T = \int_0^\infty \frac{\exp[-k^2/(2k_B T)]}{(2\pi k_B T)^{3/2}} Z_{\text{eff}}^G(k) 4\pi k^2 dk. \quad (9)$$

Finally, the latest binding energies for e^+Be, e^+Mg, and e^+Cu were used to determine ρ for Be, Mg, and Cu [50,51]. The binding energies were computed using the fixed-core stochastic variational method (FCSVM) that uses explicitly correlated gaussians to represent the wave functions for the active (valence) particles [52]. Therefore, the binding energies and annihilation rates are expected to be reasonably accurate with the accuracies for e^+-Be and e^+-Mg assessed at about 1–2% and 15%, respectively [50]. The uncertainties in the definition of the core Hamiltonian are expected to be larger for e^+Cu, however, comparisons with the completely independent configuration-interaction calculation of Dzuba *et al.* [45] suggest an overall accuracy of about 10–15%. It did not seem sensible to use a common G factor to describe the annihilation of the positron with the core and valence orbitals. The core and valence electrons have very different binding energies and, therefore, can be expected to have different enhancement factors. Since, the values of G for Ne and Ar were 2.26 and 3.02, respectively, the enhancement factor for the core, G_{core} was set to 2.5. The enhancement factor for the valence orbitals, G_{valence} was fixed by requiring the model potential and FCSVM calculation to give the same Γ for the valence subshell annihilation rate. Examination of convergence patterns for the FCSVM calculations [50,52] suggests that the relative accuracy of the FCSVM annihilation rates are comparable in size to the accuracy in the binding-energy calculations, i.e., about 1–2% for e^+-Be and about 15% for e^+Mg and e^+Cu. Matching to FCSVM annihilation rates yields G values for the valence subshells of 10.18, 13.2, and 18.2 for Be, Mg, and Cu, respectively.

III. MODEL TESTING

Having constructed a model for e^+-atom scattering it is now important to verify that the model can reproduce the salient features of the more detailed calculations. The positron-hydrogen and positron-helium systems are the ideal systems with which to benchmark the model. The cross section and Z_{eff} are known quite accurately at energies below the Ps formation threshold [7,30,35,36]. We choose to compare with the s-wave data since this permits the cleanest-possible comparison without the additional concern that dif-
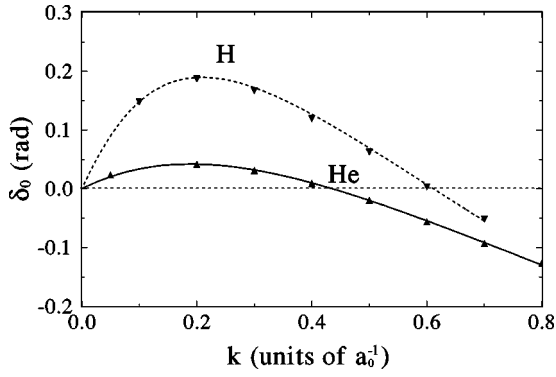
FIG. 1. The s-wave phase shift δ_0 for e^+-H (dashed line) and e^+-He scattering (solid line) as a function of k (in a_0^{-1}). Close to exact phase shifts for H [30] (down triangle) and He [35] (up triangle) and He are also included.

ferent values of ρ might be chosen for the higher partial waves.

Figure 1 shows the s-wave phase shifts for the e^+-H and e^+-He systems. It can be seen that the phase shifts for both H and He are in almost perfect agreement with the *ab initio* calculations [30,35]. Figure 2 shows the s-wave Z_{eff}^G for the e^+-H and e^+-He scattering. For helium, there is almost perfect agreement between Z_{eff}^G and the variational calculation [36]. For hydrogen, the agreement is very good below $k \lesssim 0.3 a_0^{-1}$, but $Z_{\text{eff}}^G(k)$ is slightly larger than the T-matrix calculation for the larger momenta. (It should be noted that the level of agreement for s-wave e^+-H scattering does not extend to σ_ρ and the total Z_{eff}^G. The model potential gives a very poor description of the p-wave and d-wave phase shifts and this results in a σ_ρ and Z_{eff}^G that are substantially smaller than the T-matrix calculation of Mitroy and Ryzhikh [7,30]. This problem could be eliminated by the simple expedient of having separate values of ρ for p-wave and d-wave scattering.)

The elastic cross section, σ_ρ and annihilation parameter, Z_{eff}^G, for all atoms are detailed in Tables II and III. Results for Z_{eff}^G are only given for energies below the Ps-formation

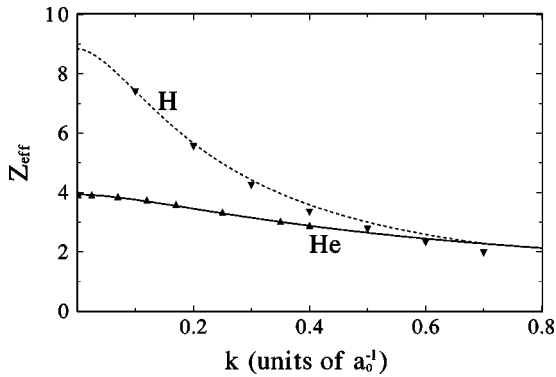FIG. 2. The s-wave annihilation parameter Z_{eff}^G for e^+-H (dashed line) and e^+-He (solid line) scattering as a function of k (in a_0^{-1}) for momenta below the Ps-formation threshold. Accurate data from *ab initio* calculations of Z_{eff} for H [7] and He [36] (up triangle) are also shown.

threshold for each atom since it is difficult to *a priori* justify the validity of the model at energies above this threshold.

The values of σ_ρ for Ne, Ar, Kr, and Xe are shown in Fig. 3 and compared with the elastic cross sections of the York group [37–39] from which the values of ρ were derived. Figure 3 shows that the present model potential is able to correctly reproduce all the features of the more complicated PO model and further validates the present model-potential approach. There have been many other calculations of positron-atom scattering cross sections that give results similar to the present model. A detailed comparison with the many other calculations and experimental measurements is not warranted since this has been done numerous times in the past [20,22,23,25,38,39].

The annihilation parameters for Ne, Ar, Kr, and Xe are plotted in Fig. 3 and compared with the $Z_{\text{eff}}(k)$ of the York group [37–39]. The purpose of this comparison was to determine whether the energy dependence of $Z_{\text{eff}}^G(k)$ was the same as the energy dependence of the PO calculations (in order to aid this comparison both sets of Z_{eff} were normalized to have the same magnitude at $k=0.1a_0^{-1}$). The shape of the $Z_{\text{eff}}^G(k)$ curves agree amazingly well with the PO calculations with some small discrepancies of order 10–20% for Kr and Xe at values of $k>0.2a_0^{-1}$. The large and rapid variations in $Z_{\text{eff}}(k)$ for Ar, Kr, and Xe near threshold are easily described with the single energy-independent enhancement factor. Tuning the value of ρ to reproduce the PO phase shifts resulted in a model hamiltonian that also reproduced the energy dependence of the PO $Z_{\text{eff}}(k)$. Although the PO calculations do not give an exact description of positron-rare gas scattering, they are realistic calculations that explicitly include electron-positron correlations. Thus, the comparisons in Fig. 3 provide further evidence that the model potential can adequately reproduce all the features expected in the real system. Further, it is possible to conjecture that the present model will reproduce the shape of the exact $Z_{\text{eff}}(k)$ curve for any atom provided ρ can be fixed by reference to the exact phase shift. The differences that occur for $k>0.2a_0^{-1}$ will not have much impact on the later discussions of the thermally averaged annihilation parameter. At reasonable temperatures, the positron momenta hardly gets higher than $0.20a_0^{-1}$ and thus the thermal average is generally dominated by annihilation at low momentum.

The ability to reproduce the energy dependence of $Z_{\text{eff}}(k)$ with a single scaling factor, G suggests it is not necessary to invoke complicated explanations involving the dynamics of the annihilating electron-positron pair to describe this energy dependence. This idea is also contained within in the analysis of Gribakin [8]. Gribakin has developed a parametrization of the low-energy behavior of $Z_{\text{eff}}(k)$, viz.,

$$Z_{\text{eff}}(k)=4\pi\rho_e\delta R_a\left(\frac{\sigma_{\text{elastic}}}{4\pi}+R_a^2+2R_a\,\text{Re}(f_0)\right) \quad (10)$$

which explicitly depends upon the behavior of the elastic cross section. The factors, ρ_e, δR_a, and R_a are free parameters that are fixed for each atom by comparison with experiment or *ab initio* calculation. The first term inside the brack-

TABLE II. The elastic cross section, σ_ρ (in units of πa_0^2) as a function of k. The cross sections at $k = 0$ were obtained by extrapolation. The cross sections are unlikely to be reliable at energies above the Ps-formation threshold.

$k(a_0^{-1})$	H	He	Be	Ne	Mg	Ar	Cu	Kr	Xe
0.0	17.5	0.926	979	1.62	183	112	574	420	8070
0.01	16.74	0.878	986.7	1.499	208.6	105.9	590.7	395.9	6310
0.02	15.81	0.824	954.8	1.363	230.1	97.82	589.8	354.6	3860
0.03	14.85	0.771	892.1	1.234	244.8	89.01	573.0	308.2	2343
0.04	13.89	0.720	811.6	1.112	254.7	80.09	545.1	262.8	1502
0.05	12.95	0.672	724.3	1.000	261.3	71.49	510.0	221.8	1019
0.06	12.03	0.625	638.1	0.896	266.1	63.45	471.2	186.3	724.7
0.08	10.32	0.540	486.0	0.713	274.8	49.48	392.2	131.4	407.1
0.10	8.797	0.463	369.0	0.561	289.3	38.39	321.6	93.89	252.4
0.15	5.811	0.310	200.4	0.304	346.9	20.65	201.9	44.09	100.4
0.20	3.834	0.205	129.2	0.179	320.0	11.82	143.6	23.79	52.61
0.25	2.575	0.136	95.49	0.145	237.4	7.453	112.5	14.92	34.10
0.30	1.791	0.0964	74.45	0.169	171.7	5.305	90.00	10.80	25.42
0.40	1.021	0.0724	46.60	0.301	101.5	3.693	56.80	7.454	16.86
0.50	0.743	0.0888	30.89	0.461	69.97	3.188	37.54	5.969	12.31
0.60	0.642	0.121	22.27	0.603	51.72	2.929	27.02	5.072	9.693
0.70	0.598	0.155	17.16	0.715	39.67	2.757	20.82	4.506	8.135
0.80	0.572	0.185	13.80	0.799	31.50	2.642	16.77	4.143	7.134
0.90	0.551	0.210	11.46	0.861	25.81	2.566	13.93	3.900	6.444
1.00	0.531	0.229	9.760	0.905	21.68	2.514	11.87	3.727	5.948

ets dominates Eq. (10) near threshold when the scattering length is large. Under these conditions, the value of Z_{eff} is just equal to the elastic cross section multiplied by the scaling factor, $\rho_e \delta R_a$.

IV. IMPLICATIONS OF THE MODEL

A. The values of G

There is a tendency for the enhancement factor G to increase as the ionization potential, I decreases. This tendency is not strictly monotonic as G for Ne is smaller than G for He. The enhancement factors are much larger for the more weakly bound metal atoms with smaller ionization potentials, being 18.2 for Cu, 10.18 for Be, and 13.2 for Mg. This trend can be explained in terms of a heuristic model that was originally advanced to describe the behavior of positronic atoms [53,54]. According to this model, the ground state of any positronic atom can be written as

$$\Psi = \alpha \Phi(\text{atom}) \phi(e^+) + \beta \Omega(\text{atom}^+) \omega(\text{Ps}). \quad (11)$$

The first of these terms represents a positron moving in the field of a polarized atom while the second term represents a Ps cluster attached to the residual ion (or atom). The relative size of α and β are determined by the ionization potential of the atomic parent. When the ionization potential is less than 0.250 hartree (the Ps binding energy) the most loosely bound electron is attached to the positron forming a Ps cluster. However, when the ionization potential is greater than 0.250 hartree, the tendency to form a Ps cluster is disrupted by the stronger attraction of the electron to the parent atom. Since

the annihilation process seems to be dominated by the $\Omega(\text{Atom}^+)\omega(\text{Ps})$ configuration [53,54] a tendency for G to increase as the ionization potential decreases is expected.

Both the scattering length and Z_{eff}^G were very sensitive to relatively small changes in the scattering potential for Kr and Xe. The calculations of the York group for these atoms only took the valence orbitals into consideration when computing the polarization potential. Some simple estimates, based on the oscillator-strength sum rule for α_d and using the Hartree-Fock-Koopman energies as a guide suggest that inclusion of the core orbitals would lead to α_d and the polarization potential for Kr and Xe increasing by 2% and 5%, respectively. A simple rescaling of V_{pol} by these amounts resulted in the threshold Z_{eff}^G increasing to 94 for Kr and 44 000 for Xe. The low-energy cross section for both of these atoms is dominated by a low-lying virtual state and a small change in the virtual-state energy leads to a large change in the threshold scattering parameters.

B. Core annihilation

When positrons annihilate with atoms, they annihilate predominantly with the valence electrons since the repulsive potential exerted by the nucleus tends to keep the positrons away from the inner regions of the atom. However a small fraction of the positrons can tunnel through the repulsive potential to annihilate with the inner electrons.

Recently, evidence of inner-shell annihilation has been obtained for krypton and xenon atoms confined in a positron trap [55]. Argon atoms were also confined in the same trap

TABLE III. The annihilation parameter Z_{eff}^G as a function of k. The thermally averaged annihilation parameter $\langle Z_{eff}^G \rangle_T$ for the noble gases is given towards the bottom of each column along with the experimental Z_{eff} obtained at room temperature.

$k(a_0^{-1})$	H	He	Be	Ne	Mg	Ar	Cu	Kr	Xe
0.00	8.841	3.951	118.9	6.118	36.05	40.15	96.40	129.4	1838
0.01	8.810	3.947	116.7	6.109	35.64	39.72	95.13	126.2	1465
0.02	8.737	3.939	111.3	6.088	35.15	38.66	92.28	118.5	926.6
0.03	8.632	3.928	103.7	6.057	34.90	37.19	88.38	108.4	585.3
0.04	8.503	3.914	94.92	6.021	35.03	35.46	83.77	97.60	392.5
0.05	8.355	3.898	85.89	5.979	35.64	33.62	78.78	87.21	279.8
0.06	8.195	3.880	77.22	5.934	36.85	31.75	73.70	77.76	209.8
0.08	7.850	3.840	62.23	5.837	41.52	28.18	64.18	62.24	132.3
0.10	7.494	3.796	50.97	5.736	49.69	25.02	56.35	50.80	92.95
0.15	6.655	3.679	35.70	5.488	76.53	19.23	45.40	34.05	52.19
0.20	5.966	3.566	30.61	5.278	76.56	15.80	42.79	26.29	38.61
0.25	5.444	3.465	28.83	5.120	60.08	13.86	42.03	22.62	33.48
0.30	5.068	3.379	27.27	5.017	47.24	12.83	39.87	20.94	31.35
0.40	4.636	3.262	23.59	4.957		12.13		19.88	29.46
0.50	4.468	3.208	20.98	5.045		12.14		19.72	28.43
0.60	4.431	3.206		5.225		12.33		19.81	28.06
0.70	4.458	3.240		5.457		12.60		20.08	28.20
0.80		3.298		5.714		12.91		20.50	28.60
0.90		3.371		5.984		13.27		20.99	29.11
1.00		3.454		6.260		13.64		21.52	29.64
$\langle Z_{eff}^G \rangle_T$		3.90		5.98		33.8		90.1	401
Z_{eff}(expt[a])		3.94		5.99		26.8		65.7	400-450
Z_{eff}(expt[b])						33.8		90.1	401
$\langle Z_{eff}^G \rangle_T$[c]		3.82		6.98		30.5		56.3	200.4

[a]Measurements of UCL group [48,49].

[b]Measurements of San Diego group [4,47].

[c]Thermally averaged values derived from York group calculations [15,37,39].

but there was no conclusive evidence for inner-shell annihilation.

Table IV gives the relative contribution to Z_{eff} from the two outer shells with quantum numbers n and $(n-1)$, respectively. The values of Z_{eff}^G were computed at $k = 0.05a_0^{-1}$ although it should be noted that the relative con-

tribution changed slowly with energy. The data in the static-field approximation [55] are equivalent to the current model calculations with $V_{pol} \equiv 0$ and $G = 1$ (the values reported in Ref. [55] have been verified). The inclusion of the polarization potential and enhancement factor results in a great increase in Z_{eff} (as previously noted [9]). Besides the great
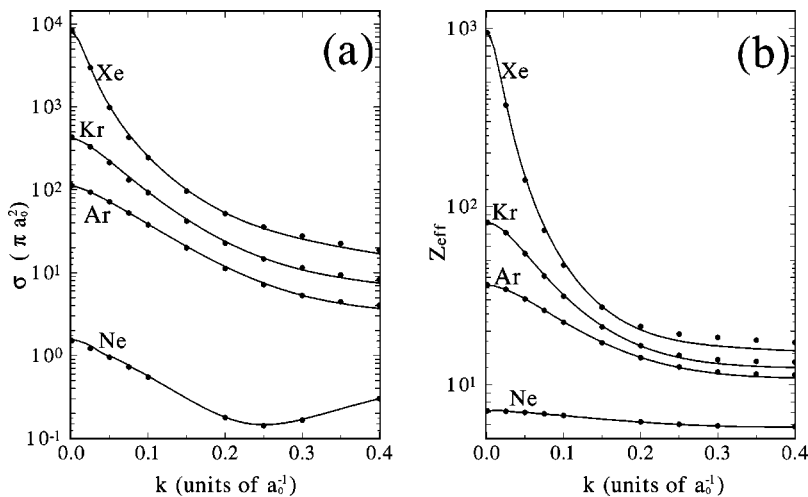

FIG. 3. The elastic cross section σ_ρ (a) (in units of πa_0^2) and annihilation parameter Z_{eff}^G (b) for Ne, Ar, Kr, and Xe as a function of k (in a_0^{-1}). The Z_{eff} and elastic cross section for the polarized orbital calculations of the York group [37–39] are shown as a discrete set of points. It should be noted for purpose of comparison that the Z_{eff}^G in (b) have been renormalized to have the same magnitude as the York group data at $k = 0.1a_0^{-1}$.

TABLE IV. Respective contributions to Z_{eff} from the n and $n-1$ shells. The experimental values were taken at room temperature while the calculated values were obtained at $k=0.05a_0^{-1}$. The respective contributions are given as a fraction that must sum to 1. The net Z_{eff} including contributions from all shells is also given.

Shells	Ar	Kr	Xe
Static potential: $\alpha_d=0$, $G=1$			
$ns+np$	0.989	0.968	0.952
$(n-1)s+(n-1)p+(n-1)d$	0.011	0.032	0.048
Z_{eff} (net)	0.761	0.718	0.671
Fit to experiment [55]			
$ns+np$	>0.998	0.987	0.976
$(n-1)s+(n-1)p+(n-1)d$	<0.002	0.013	0.024
Z_{eff}^G			
$ns+np$	0.982	0.944	0.897
$(n-1)s+(n-1)p+(n-1)d$	0.018	0.056	0.103
Z_{eff} (net)	33.6	87.2	280

TABLE V. The real part of the scattering length A_r (in a_0), the threshold value of Z_{eff}^G and the Z_{eff} at thermal energies ($T=293$ K) are tabulated as a function of α_d (in a_0^3) for a model argon atom.

$\alpha_d(a_0^3)$	$A_r(a_0)$	Z_{eff}^G	Z_{eff}^G/A_r^2	$\langle Z_{\text{eff}}^G\rangle_T$
4.0	0.127	4.77	295	4.71
6.0	−0.735	7.54	14.0	7.25
8.0	−1.92	13.0	3.51	12.1
10.0	−3.74	25.3	1.81	22.4
11.1	−5.30	40.1	1.43	33.8
12.0	−7.13	62.9	1.24	49.7
13.0	−10.4	117.0	1.09	82.4
14.0	−16.6	274.1	0.993	151.8
15.0	−34.2	1086	0.927	328.1
15.5	−66.2	3970	0.905	524.5
15.9	−229	46867	0.890	804.4
16.5	91.0	7244	0.875	672.6
17.0	43.1	1607	0.866	453.1
17.5	28.6	704.4	0.863	318.7
18.0	21.5	399.9	0.864	233.5
19.0	14.6	185.6	0.877	139.0
20.0	11.0	110.5	0.906	92.3
22.0	7.40	55.9	1.02	51.0
24.0	5.41	36.3	1.24	34.3
26.0	4.06	27.1	1.64	26.5
28.0	3.00	22.2	2.45	23.1
30.0	2.11	19.4	4.36	24.2

increase in Z_{eff} there has also been an increase in the relative contribution from the $(n-1)$ shell. The inclusion of the polarization potential makes the disagreement between theory and experiment worse as the static-field approximation already overestimates the relative contribution from core annihilation.

This disagreement is not too severe when the origin of the experimental annihilation fractions are examined. The experimental annihilation ratio was deduced by comparing the experimental Doppler broadening spectrum with the results of a static-field calculation. However, the static-field calculation does not give an accurate description of the scattering process and underestimates the value of Z_{eff} for Xe by a factor of 100. The core-annihilation ratio of 0.024 for Xe derived from the fit to the static-field calculation is probably less accurate than the present model-potential calculation. In addition, the static-field calculation uses nonrelativistic Hartree-Fock wave functions to model the structure of the xenon atoms. Relativistic effects are known to substantially modify the radial and momentum electron densities in xenon [56,57]. In addition, it must be mentioned that experiments performed by the UCL/Norwich group [58] obtained substantially wider Doppler profiles for Ar, Kr, and Xe. To summarize, the magnitude of the theoretical uncertainties associated with the determination of the core-annihilation fraction are so large that one could seriously question whether there is any evidence for the existence of the core-annihilation process itself.

C. Increasing the scattering length

It is interesting to explore the relationship between the elastic cross section and the annihilation parameter. The e^+-Ar system was used as a representative system and the parameter α_d was varied in a systematic manner. Increasing α_d leads to a more attractive potential and, therefore, a negative scattering length that increases in magnitude. When α_d becomes sufficiently large, the model Hamiltonian supports a bound state, and the scattering length changes sign. Decreas-

ing the polarizability results in a scattering length that becomes less negative and eventually approaches zero. This is also consistent with an effective range analysis of Ps-p scattering presented in Ref. [59].

The relationship between the threshold Z_{eff}^G and the scattering length (A_r) can be seen in Table V where both of these quantities are tabulated as a function of α_d. A noticeable feature of Table V is smooth behavior of Z_{eff}^G/A_r^2 when α_d changes from $11a_0$ to $25a_0^3$. Over this range, the scattering length changes from $-5.3a_0\rightarrow-\infty$, and once the threshold for binding is reached from $\infty\rightarrow5a_0$. When A_r is close to the threshold for binding the ratio is almost constant. This implies an almost direct proportionality between the threshold cross section and Z_{eff}^G. These calculations demonstrate that the dynamical interactions that lead to a large and strongly peaked elastic cross section also inevitably lead to a large Z_{eff} at threshold. It will be demonstrated in the next section that this is a consequence of the normalization condition that relates the scattering wave function in the inner and asymptotic regions. The present model calculations and the results in Table V suggest that the large threshold values of Z_{eff} for Kr and Xe are the consequence of a large scattering length and not the result of a very large enhancement factor or exceptionally strong electron-positron correlations. We note in passing that Jain and Thompson [60] previously suggested that mundane scattering processes were responsible for the large Z_{eff} in methane.

The thermally averaged Z_{eff}^G, i.e., $\langle Z_{\text{eff}}^G\rangle_T$, at room temperature ($T=293$ K) is also given in Table V. There is a

tendency for $\langle Z_{\text{eff}}^G \rangle_T$ to approach a constant value for larger values of the scattering length. This is consistent with the analysis of Gribakin and co-workers [8,9].

D. The pole approximation

A number of these atoms are characterized by having a bound state or a large scattering length that signifies the existence of a virtual state. Such systems can be characterized by the pole approximation, i.e., the S matrix close to threshold is given by [61,62]

$$\mathbf{S}_{\text{pole}}(k) = \frac{1 - ik/\kappa}{1 + ik/\kappa}, \qquad (12)$$

where $\kappa = \kappa_r + i\kappa_i$ and κ_r, κ_i are real parameters that denote the position of the pole in the complex k plane. The pole position $ik = -\kappa$ is not a pure imaginary number even for a physical bound state since these systems can decay by electron-positron annihilation. In the framework of absorptive-potential theory this process can be taken into account using a nonunitary **S** matrix in Eq. (12). The parameter κ_r is positive for a real bound state and negative for a virtual state. The value of the parameter κ_i responsible for the nonunitarity is determined by the absorptive interaction and is very small since the annihilation cross section is very small. In the case of a real bound state the parameters κ_r and κ_i are related to the real ε_r, and imaginary ε_i part of the energy by

$$\kappa_r \approx \sqrt{2|\varepsilon_r|}, \qquad \kappa_i \approx -\frac{\varepsilon_i}{\sqrt{2|\varepsilon_r|}}. \qquad (13)$$

The above expressions assume that $\varepsilon_r \gg \varepsilon_i$ and all subsequent expression utilize this assumption. The imaginary part of the energy (in hartree) is related to the annihilation rate, Γ_{SI} in s^{-1} by the identity

$$\varepsilon_i = -2.418\,88 \times 10^{-17} \frac{\Gamma_{SI}}{2}. \qquad (14)$$

The parameter κ_i is positive for a physical bound state.

The formula (12) for the $\mathbf{S}_{\text{pole}}$ matrix leads to the following expression for the (complex) phase shift:

$$\delta_0(k) + i\mu_0(k) = -\arctan\left(\frac{k}{\kappa_r}\right) - i\frac{k\kappa_i}{k^2 + \kappa_r^2}. \qquad (15)$$

The real part of the phase shift, δ_0 gives the well-known expression for the s-wave scattering cross section if the system has a shallow level (real or virtual),

$$\sigma_{\text{elastic}}(k) = \frac{4\pi}{k^2 + \kappa_r^2}. \qquad (16)$$

The spin-averaged absorption cross section is given by

$$\sigma_{\text{abs}} = \frac{\pi}{k^2}(1 - |\mathbf{S}|^2) = \frac{\pi}{k^2}[1 - \exp(-4\mu_0)]. \qquad (17)$$

In most circumstances, the imaginary part of the phase shift is small, therefore, using Eq. (4), and simplifying Eq. (17) it follows that

$$Z_{\text{eff}}(k) = \frac{4\mu_0(k)}{cr_0^2 k} = \frac{1}{cr_0^2} \frac{4|\kappa_i|}{(k^2 + \kappa_r^2)}. \qquad (18)$$

Goldanskii and Sayasov [63,64] and Dzuba et al. [9,10] had previously obtained expressions for $Z_{\text{eff}}(k)$ with the same energy dependence as Eq. (18). However, they did not relate the magnitude of Z_{eff} directly to κ_i and both of these earlier works contain additional arbitrary parameters that multiply the form factor. Equation (10) due to Gribakin [8] represents an extension of the method of Dzuba et al. [9,10] and has a wider region of validity. In circumstances where the pole approximation is valid, Eq. (10) due to Gribakin and Eq. (18) have the same momentum dependence.

For some applications it is desirable to express the pole parameters κ_i and κ_r in these formulas in terms of the real and imaginary scattering lengths. For a shallow real or virtual state the relation between the pole position and complex scattering length $A = A_r + iA_i$ is

$$\kappa_i + i\kappa_r = \frac{1}{A_r + iA_i}, \qquad (19)$$

from which it follows that

$$A_r = \frac{1}{\kappa_r}, \qquad A_i = -\frac{\kappa_i}{\kappa_r^2}. \qquad (20)$$

$$\kappa_r = \frac{1}{A_r}, \qquad \kappa_i = -\frac{A_i}{A_r^2}. \qquad (21)$$

Using these relations, one can immediately write Eq. (18) as

$$Z_{\text{eff}}(k) = \frac{4|A_i|}{cr_0^2(1 + A_r^2 k^2)}, \qquad (22)$$

while the threshold elastic cross section $\sigma_{\text{elastic}} = 4\pi A_r^2$ as usual. For atoms with a single valence electron, such as H or Cu, the factor A_i is obtained by spin averaging the singlet and triplet A_i. Values for A_r, A_i, κ_r, κ_i, ε_r, and ε_i derived from the threshold Z_{eff}^G and σ_ρ are given in Table VI for all systems.

Equations (18) and (22) also provide some justification for the use of an energy-independent enhancement factor G. In Eq. (22), the energy dependence is largely determined by A_r while the magnitude is determined by the multiplying factor A_i. Comparison of formulas (16) and (22) show that Z_{eff} and the elastic section (16) are proportional, viz.,

$$\frac{Z_{\text{eff}}(k)}{\sigma_{\text{elastic}}(k)} = \frac{|A_i|}{\pi cr_0^2 A_r^2}. \qquad (23)$$

While this expression shows that $Z_{\text{eff}}/\sigma_{\text{elastic}}$ should be independent of energy for small k, it does not explain why A_i/A_r^2 should be constant as $A_r \to \infty$. The behavior seen in

TABLE VI. Scattering parameters associated with the pole approximation to the s-wave phase shift. The parameters were derived from the scattering length and threshold Z_{eff}^G. All quantities are in atomic units with the exception of the half-width of the bound or virtual state that is in units of 10^9 s^{-1}. The notation a^b is used to represent $a \times 10^b$. The values of κ_i^* were computed directly from the $e^+\text{Be}$, $e^+\text{Mg}$, and $e^+\text{Cu}$ binding energies and annihilation rates.

Quantity	H	He	Be	Ne	Mg	Ar	Cu	Kr	Xe
A_r	-2.10	-0.483	15.6	-0.640	6.48	-5.30	11.8	-10.3	-45.0
κ_r	0.476	2.07	0.0645	1.56	0.154	0.189	0.0847	0.0971	0.0222
ε_r	0.113	2.14	$0.002\,08$	1.22	0.0119	0.0178	$0.003\,59$	$0.004\,71$	$0.000\,247$
A_i	8.64^{-7}	3.84^{-7}	1.16^{-5}	5.94^{-7}	3.50^{-6}	3.90^{-6}	9.37^{-6}	1.26^{-5}	1.79^{-4}
κ_i	1.96^{-7}	1.65^{-6}	4.81^{-8}	1.45^{-6}	8.33^{-8}	1.39^{-7}	6.73^{-8}	1.21^{-7}	8.82^{-8}
ε_i	9.33^{-8}	3.41^{-6}	3.10^{-9}	2.27^{-6}	1.29^{-8}	2.62^{-8}	5.70^{-9}	1.18^{-8}	1.96^{-9}
$\Gamma/2$	3.86	141	0.128	93.7	0.531	1.08	0.236	0.490	0.0810
κ_i^*			6.43^{-8}		6.92^{-8}		6.91^{-8}		

Table V requires an approach that goes beyond the simple pole approximation. This is now done.

In its most general and simplest form, the (s-wave) annihilation parameter can be written as

$$Z_{\text{eff}} = \int_0^\infty |P_k(r)|^2 W(r) dr, \tag{24}$$

where $P_k(r)$ is a normalized solution of the Schrödinger equation,

$$\left(-\frac{1}{2}\frac{d^2}{dr^2} + V_{\text{dir}}(r) + V_{\text{pol}}(r) \right) P_k(r) = \frac{k^2}{2} P_k(r). \tag{25}$$

The annihilation operator $W(r)$ contains all factors of r_0, c, and the atomic electron density. It is a singularity free and positive definite operator that is also short ranged. The operator $W(r)$ is very weak in magnitude and does not have to be included in the Hamiltonian when $P_k(r)$ is generated.

A cut-off radius r_s is defined with the property that both the scattering potential and annihilation operator are zero outside this radius. When $r > r_s$, the normalized scattering wave function $P_k(r)$ is given by

$$P_k(r) = \frac{\sin[kr + \delta_0(k)]}{k}, \quad r > r_s, \tag{26}$$

while Z_{eff} is now obtained over a restricted integration range, viz.,

$$Z_{\text{eff}}(k) = \int_0^{r_s} |P_k(r)|^2 W(r) dr. \tag{27}$$

The radial wave function $P_k(r)$ can be written as

$$P_k(r) = N(k) F_k(r), \tag{28}$$

where $F_k(r)$ is the regular solution of the Schrödinger equation with the boundary conditions $F_k(0) = 0$, $F_k'(0) = 1$. Since the boundary conditions do not contain k, the solution $F_k(r)$ varies slowly with k. Most of the k dependence of

$P_k(r)$ comes from the factor $N(k)$ that arises from the asymptotic normalization condition.

The normalization condition is obtained from the requirement that the wave function (and its derivative) be continuous at the matching radius r_s. Therefore,

$$N(k) = \frac{\sin[kr_s + \delta_0(k)]}{kF_k(r_s)} \tag{29}$$

and

$$P_k(r) = \frac{\sin[kr_s + \delta_0(k)]}{kF_k(r_s)} F_k(r). \tag{30}$$

For small momenta such that $kA_r \ll 1$ and $kr_s \ll 1$, it is possible to rewrite this function as

$$P_k(r) = \frac{(r_s - A_r)}{F_k(r_s)} F_k(r). \tag{31}$$

Equation (27) can be now rewritten as

$$Z_{\text{eff}}(k) = \frac{(r_s - A_r)^2}{|F_k(r_s)|^2} \int_0^{r_s} |F_k(r)|^2 W(r) dr. \tag{32}$$

The ratio of $\int|F_k(r)|^2 W(r) dr$ and $|F_k(r_s)|^2$ on the right-hand side of Eq. (32) will depend only weakly on energy, and in addition it will change slowly for small variations in the scattering potential. However, when the scattering length is large, small changes in the scattering potential can lead to large changes in A_r. In these circumstances, the changes in Z_{eff} for different potentials are largely driven by the $(r_s - A_r)^2$ normalizing factor. Therefore, the ratio Z_{eff}/A_r^2 should be roughly constant as $A_r \to \infty$. Although the derivation above assumes a relatively simple scattering wave function, Eq. (32) does not rely on a specific form for the scattering wave function in the interior region. It is only necessary that the total scattering wave function collapse to a simple product form for $r \geq r_s$. Therefore, the limiting behavior implied by Eq. (32) is expected to be true under quite general circumstances.
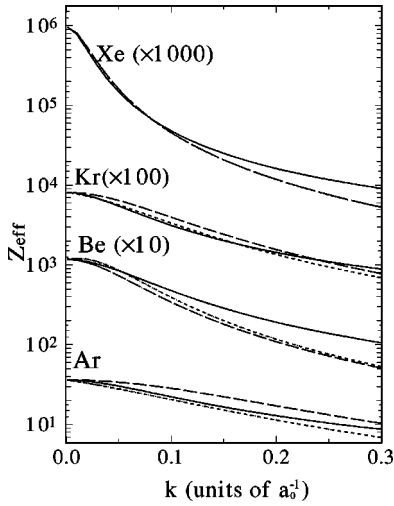
FIG. 4. A comparison of $Z_{eff}^G(k)$ versus the pole approximation for Ar, Be, Kr, and Xe. A solid line was used for $Z_{eff}^G(k)$. The simple pole approximation was represented by a long dashed line and the polarizability-corrected pole approximation was represented as a short dashed line (these two approximations were identical for Xe). Note that κ_r in the pole approximation was obtained directly from the zero-energy phase shift and not treated as a fitting parameter.

The pole approximation to Z_{eff} derived from the **S** matrix is expected to be reliable when both κ and k are close to the threshold. In Fig. 4, $Z_{eff}^G(k)$ and the pole approximation given by Eq. (18) are plotted. The pole approximation is quantitatively accurate for Xe (for $k < 0.1a_0^{-1}$) and for Kr and Ar gives the general shape of $Z_{eff}^G(k)$ but is not quantitatively accurate. However, the long-range polarizability can be included in a modified pole approximation

$$\mathbf{S}_{pole}(k) = \frac{1 - ik\left(A_r + \frac{\pi\alpha_d k}{3} + iA_i\right)}{1 + ik\left(A_r + \frac{\pi\alpha_d k}{3} + iA_i\right)}. \qquad (33)$$

When this is done, Z_{eff} becomes

$$Z_{eff}(k) = \frac{4|A_i|}{cr_0^2\left(\left(1 - \frac{\alpha_d\pi k}{3A_r}\right)^2 + A_r^2 k^2\right)}. \qquad (34)$$

This inclusion of the linear term generally improves the accuracy of Z_{eff} for small k and this is clearly seen from Fig. 4 where Eq. (34) is plotted and compared with Z_{eff}^G. Equation (34) is presented since it generally gives an improved description of $Z_{eff}(k)$ at lower k without any additional parameters. There is no perceptible difference between Eqs. (18) and (34) for xenon ($A_r = -45a_0$). For establishing general trends Eq. (18) is preferred due to its simpler analytic form. We note a more complete analysis of the structure of the S matrix in the presence of a polarization potential has been presented elsewhere in a description of Ps-p scattering [59].
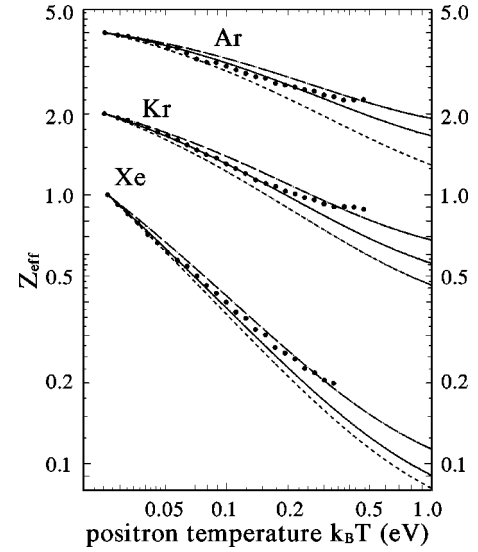

FIG. 5. The annihilation parameter Z_{eff}^G as a function of positron temperature (in eV) for Ar, Kr, and Xe. All experimental and theoretical curves for a given atom are normalized to a common value at the lowest temperature. The solid curve represents the best fit to the data while the upper and lower dashed curves show the calculations with minimum and maximum scattering lengths that are compatible with data. For Ar the three curves have scattering lengths of $-4.6a_0$, $-5.6a_0$, and $-6.6a_0$. For Kr the three curves have scattering lengths of $-8.3a_0$, $-10.3a_0$, and $-12.3a_0$. For Xe the three curves have scattering lengths of $-40a_0$, $-56a_0$, and $-71a_0$.

E. Temperature dependence

To a first approximation, the energy dependence of $Z_{eff}(k)$ is roughly independent of κ_i or A_i. This raises the possibility that temperature dependence of $\langle Z_{eff}\rangle_T$ can be used to determine scattering parameters such as the scattering length.

Accordingly the parameter ρ, and therefore A_r were varied for a series of calculations on Ar, Kr, and Xe and $\langle Z_{eff}\rangle_T$ was evaluated by integrating Eq. (9). The function $Z_{eff}^G(k)$ was computed at about 120 points for $k \in [0.0, 1.0]$. A natural cubic spline was used to convert this discrete set of points into a continuous function for the integration. For $k > 1.0a_0^{-1}$ $Z_{eff}^G(k)$ was set equal to its values at $k = 1.0a_0^{-1}$. Generally the Maxwellian average was dominated by the low k values. For example, contributions from $k < 0.2a_0^{-1}$ comprise more than 99.9% of the Ar $\langle Z_{eff}\rangle_T$ for positron temperatures less than 0.1 eV.

The results of the calculations for $\langle Z_{eff}^G\rangle_T$ are shown Fig. 5 and compared with the data of Kurz *et al.* [65]. As the data of Kurz *et al.* [65] are not absolute, the curves for the different atoms have been normalized to a common point and thus the comparisons are independent of G. Three curves were drawn for each atom. The "middle" curve represents the best fit to the data for positron temperatures less than 0.1 eV. The other two curves correspond to situations with the minimum and maximum A_r values. For Kr, the $\langle Z_{eff}^G\rangle_T$ given in Table III gives an almost perfect fit to the data for $k_BT < 0.2$ eV and suggests a scattering length of $-10.3 \pm 2.0a_0$.

The fits for Ar and Xe were not of the same quality as there was a tendency for the experimental data to have a

slightly different shape. The values of ρ had to be changed for Ar and Xe (giving scattering lengths of $-5.6a_0$ and $-56a_0$, respectively) in order to get a reasonable fit to the experimental data. This is a potential cause for concern since the fits of the convoluted $Z_{\mathrm{eff}}(k)$ of the York group for Ar and Xe [38,39] presented in Kurz *et al.* [65] were excellent (excluding $k_B T > 0.2$ eV). However, there were some small but significant numerical errors present in the thermal averaging as performed by Kurz *et al.* [66] and thus their convolutions of the York group cross sections can be discounted. When we applied our thermal averaging procedures to the tabulated $Z_{\mathrm{eff}}(k)$ of the York group we found excellent agreement with the $\langle Z_{\mathrm{eff}}^G \rangle_T$ curves generated using the Z_{eff}^G of Table III.

The temperature dependence of Z_{eff} was also measured in a Xe-H_2 mixture by the UCL group [49]. A quick examination of Fig. 5 of Ref. [49] suggests that problems exist with this data. The data are suggestive of a $\langle Z_{\mathrm{eff}} \rangle_T$ curve that decreases as $\langle Z_{\mathrm{eff}} \rangle_T \propto T^{-1.3}$. However, the present calculations (e.g., comparison with the San Diego data in Fig. 5) and the analysis of Dzuba *et al.* [9] suggest that such a rapid decrease is not possible. One consequence of the thermal average of Eq. (18) [9] is a $\langle Z_{\mathrm{eff}} \rangle_T$ that can decrease no faster than $1/T$. It may be relevant that the data of the UCL group were obtained at relatively high gas densities (4 amagat) where they acknowledge clustering effects may be important.

V. Z_{eff} FOR METAL VAPORS

Systematic tabulations of Z_{eff} for a number of gases have shown that a number of gases obey the empirical formula [67]

$$\ln(Z_{\mathrm{eff}}) = B|I - E_{Ps}|^{-1}, \tag{35}$$

where B is an empirical constant and E_{Ps} is the Ps binding energy. Using Eq. (35) as a guide, there have been speculations that metal vapors such as Zn and Cd could have threshold Z_{eff} of order 10^6 to 10^7 [68]. With positron binding energies and annihilation rates known reasonably accurately for a number of metals, it is possible to derive quick estimates of the threshold cross section and Z_{eff}.

A. Application of the pole approximation

Before using the model potential to determine the threshold cross section and phase shift it is instructive to apply the pole approximation to this problem. The real part of the scattering length and the threshold Z_{eff} derived from Eqs. (18) and (21) are

$$A_r = \frac{1}{\sqrt{2|\varepsilon_r|}}, \tag{36}$$

$$Z_{\mathrm{eff}}(k=0) = \frac{\sqrt{2}|\varepsilon_i|}{cr_0^2\sqrt{|\varepsilon_r|^3}} = \frac{\Gamma}{cr_0^2\sqrt{2|\varepsilon_r|^3}}$$

$$= 4.401\,53 \times 10^{-11} \frac{\Gamma_{SI}}{\sqrt{|\varepsilon_r|^3}}. \tag{37}$$

TABLE VII. The scattering length (in a_0) and threshold Z_{eff} and for Be, Mg, and Cu estimated using the pole approximation and the model potential.

Atom	Pole approximation		Model potential	
	A_r	Z_{eff}	A_r	Z_{eff}^G
Be	12.6	104	15.6	118.9
Mg	5.66	21.6	6.48	36.0
Cu	9.45	60.8	11.8	96.4

In this equation, ε_r is expressed in hartree while the annihilation rate given in s^{-1} is denoted Γ_{SI}. This shows clearly that the threshold Z_{eff} is largest for systems that have small binding energies, ε_r. Systems with a relatively large positron binding energy are not expected to have a particularly large Z_{eff} since ε_i has an upper limit of 2.5×10^{-8} hartree (assuming the maximum Γ is $\approx 2 \times 10^9\,\mathrm{s}^{-1}$).

The application of Eq. (37) to Be, Mg, and Cu (results tabulated in Table VII) show that the threshold Z_{eff} ranges between 20 and 100. Although the effective-range analysis is approximate, the errors associated with the analysis are small enough to rule out the speculative estimates of 10^6 to 10^7 [68].

The ratio Z_{eff}/A_r^2 is most easily evaluated by combining Eqs. (36) and (37), viz.,

$$\frac{Z_{\mathrm{eff}}}{A_r^2} = \frac{4\kappa_i}{cr_0^2} = \frac{2\Gamma}{cr_0^2\sqrt{2|\varepsilon_r|}} = 8.803\,06 \times 10^{-11} \frac{\Gamma_{SI}}{\sqrt{|\varepsilon_r|}}. \tag{38}$$

The constancy of this ratio when the pole approximation is valid implies that the annihilation rate is proportional to the square root of the binding energy, i.e., $\Gamma \propto \sqrt{\varepsilon_r}$. This relation should be true for weakly bound states and can be demonstrated using relatively simple arguments. The wave function for an $L=0$ positron bound state can be split into two parts. Let $\phi_1(r)$ be the wave function in the inner region of the atom, while $\phi_2(r)$ is the wave function in the region, $r > r_s$ where the potential and electron density are zero. The function $\phi_2(r)$ has the form

$$\phi_2(r) \sim \exp(-\kappa_r r), \tag{39}$$

where $\kappa_r = \sqrt{2|\varepsilon_r|}$ and $\phi_2(r)$ must be continuous with $\phi_1(r)$ at $r = r_s$. The annihilation rate is

$$\Gamma = \frac{\int_0^{r_s} \phi_1^2(r)W(r)dr}{\int_0^{r_s} \phi_1^2(r)dr + \phi_1^2(r_s)\exp(2\kappa_r r_s)\int_{r_s}^{\infty} \phi_2^2(r)dr}, \tag{40}$$

which can be written as

$$\Gamma = \frac{\int_0^{r_s} \phi_1^2(r) W(r) dr}{\int_0^{r_s} \phi_1^2(r) dr + \phi_1^2(r_s)/(2\kappa_r r_s)}. \tag{41}$$

The second term in the denominator, i.e., $\phi_1^2(r_s)/(2\kappa_r r_s)$ will dominate the normalization condition for shallow levels satisfying $k_r r_s \ll 1$. Succinctly, the long tail of the wave function begins to provide the bulk of the normalization integral. When this happens, the simplified form for Γ is

$$\Gamma \approx (2\kappa_r r_s) \frac{\int_0^{r_s} \phi_1^2(r) W(r) dr}{\phi_1^2(r_s)}. \tag{42}$$

This demonstrates that the annihilation rate Γ is clearly proportional to κ_r (i.e., $\sqrt{2\varepsilon_r}$) for small κ_r. The factor containing the wave function $\phi_1(r)$ can be expected to vary quite slowly as the changes in the potential lead to small absolute changes (but large relative changes) in the binding energy. Equation (42) can be expected to be generally valid since the positron wave function can take any form in the inner region.

Equation (42) is consistent with the evidence from an investigation of the (m^+, e^-, e^+) system [69]. The e^+ binding energy and annihilation rate of this system changed as the m^+/m_e mass ratio was varied from 1.40 to 1.634. Over this mass range the binding energy changed by five orders of magnitude, i.e., from 8.6×10^{-4} to 6.6×10^{-9} hartree. However, the $\Gamma/\sqrt{\varepsilon_r}$ ratio was almost constant and only varied from 7.7×10^9 to 8.4×10^9 s^{-1} a_0. These mass ratios correspond to physical situations where the positron is weakly bound to the (m^+, e^-) model atom and largely found outside the atom.

B. Model-potential calculation

While the pole approximation gives the first approximation to the threshold Z_{eff}, there are long-range polarization potentials in the Hamiltonian that can limit its range of validity. More reliable estimates of the threshold behavior can be obtained by directly solving the model Schrödinger equation for the values of ρ and G given in Table I. Results of these calculations are detailed in Tables II and III.

The scattering length (real part), and the annihilation parameter, $Z_{\text{eff}}^G(k=0)$ for Be, Mg, and Cu are listed in Table V. (Explicit calculations for Zn and Cd have not been done since the e^+ binding energies are far from converged. However, the threshold Z_{eff} are expected to lie between those of Be and Mg.) The values obtained by direct solution of the Schrödinger equation are generally of order 20–30 % different from those given by the pole approximation. While the pole approximation can be used to establish general trends it is not accurate enough for precise numerical work.

The model-potential values for the annihilation parameter confirm the analysis using the pole approximation, i.e., Z_{eff} is

only moderately large at threshold with values ranging from 35 to 120. The energy dependence of Z_{eff}^G for magnesium is unusual since it starts to increase just above threshold. This behavior is largely due to the $L=1$ partial wave. At $k = 0.15a_0^{-1}$ the s wave Z_{eff}^G was 19.1 while that of the p wave is 57.2. This increase in Z_{eff}^G is associated with a large p-wave phase shift, $\delta_1(k=0.15) = 0.645$. Indeed the momentum dependence of the p-wave phase shift suggests that the potential is showing the first signs of supporting a bound state.

C. The value of κ_i

Values of κ_i are listed in Table VI for all systems. Three of these systems, H, He, and Ne have small scattering lengths and, therefore, cannot be expected to obey a pole approximation. The other atoms have values of κ_i that range from $4.8^{-8}a_0^{-1}$ to $1.25^{-7}a_0^{-1}$. This is a small range considering that the threshold Z_{eff} changes by a factor of 30.

This variation in κ_i can be made even smaller if the best possible information is used to compute κ_i. The value of κ_i for Be, Mg, and Cu can be directly computed from the binding energy and annihilation rate of e^+-Be, e^+-Mg, and e^+-Cu. The values of κ_i for Be, Mg, and Cu were $6.43 \times 10^{-8}a_0^{-1}$, $6.55 \times 10^{-8}a_0^{-1}$, and $6.91 \times 10^{-8}a_0^{-1}$, respectively. In addition, the (m^+, e^-, e^+) system yields κ_i between 6.6×10^{-8} and 7.2×10^{-8}, for $m^+/m_e \geq 1.40$. The heavier rare-gas values of κ_i were $13.9 \times 10^{-8}a_0^{-1}$, $12.1 \times 10^{-8}a_0^{-1}$, and $8.82 \times 10^{-8}a_0^{-1}$ for Ar, Kr, and Xe, respectively. These similarities suggest that different atoms with similar structures will have roughly the same value of κ_i and this conjecture could be useful in relating cross sections and Z_{eff}.

As an example, we now give an estimate of the maximum possible value for $\langle Z_{\text{eff}} \rangle_T$ expected in a simple collision (i.e., one without contributions arising from resonances due to vibrational or rotational couplings present in molecules). Taking $1.2 \times 10^{-8}a_0^{-1}$ as the maximum reasonable κ_i makes it possible to evaluate Eq. (21) of Ref. [8] for arbitrary κ_r or T. The maximum possible value for $\langle Z_{\text{eff}} \rangle_T$ is 1300. Previously, Dzuba *et al.* [9,10] and Gribakin [8] have suggested maximum possible room temperature $\langle Z_{\text{eff}} \rangle_T$ ranging between 200 and 1000. The present result confirms and strengthens the idea that $\langle Z_{\text{eff}} \rangle_T$ has an upper limit that depends on temperature for systems that have simple collisions with positrons.

It is also instructive to analyze the results of a large-scale Schwinger variational calculation of e^+-C_2H_2 [11] scattering by the Campinas group. At an energy of 0.0001 eV the elastic cross section was $1.47 \times 10^5 \pi a_0^2$ while Z_{eff} was 1.4×10^5. These imply a scattering length of $-225a_0$ and a threshold Z_{eff} of 1.9×10^5. The derived value of κ_i was $3.6 \times 10^{-7}a_0^{-1}$. This value of κ_i is three times higher than the κ_i for any of the atoms with $|A_r| > 5a_0$. The relatively large value of κ_i for C_2H_2 immediately suggested that the Schwinger variational calculations were simply wrong.

Accordingly, other calculations of Z_{eff} by the Campinas group were scrutinized for evidence to either support or refute this contention. This additional evidence also suggests that their calculations are indeed incorrect. First, their calcu-

lated Z_{eff} for N_2 is about three times larger than experiment [11]. Second, they have calculated Z_{eff} and the elastic cross section for positron-helium scattering [12]. Here, their calculation gave a threshold Z_{eff} of 4.2, in reasonable agreement with the expected value of 3.95 [36,48]. However, not too much credence can be given to this result since their threshold cross section of about $0.25\pi a_0^2$ is about 3.5 times smaller than the (close to exact) variational cross section [35] of $0.95\pi a_0^2$. Therefore, their computed value of Z_{eff}/A_r^2 is too large by a factor of 3 to 4. Finally, they have also computed Z_{eff} for e^+-He scattering in a static model with no polarization. For momenta from threshold to $k=0.6a_0^{-1}$ they report values of Z_{eff} ranging from 1.2 to 2.3. Running the current program for helium with $\alpha_d=0$ and $G=1$ gives values of Z_{eff}^G that range from 0.689 at threshold to 0.863 at $k=0.6a_0^{-1}$. (It is also noted that Dzuba *et al.* [9] have also done calculations in this model and report a value of 0.69 close to threshold). The discrepancy in Z_{eff} for two notionally equivalent models provides compelling evidence of an error in the Z_{eff} calculations of the Campinas group. One diagnostic that can be useful in validating the programs used to compute Z_{eff} is to run calculations with all the interaction potentials set to zero and check whether Z_{eff} is equal to the number of electrons in the atom (or molecule). This test was used for the present calculation and in an earlier momentum-space T-matrix calculation [7]. These concerns have been communicated to the Lima *et al.* They have since carefully analyzed their program and have discovered a simple scaling error in their calculation of Z_{eff}. Their published Z_{eff} for He was too large by a factor of about 2, while their calculation of C_2H_2 is most likely too big by an even larger factor [70].

This analysis is relevant to the current debate [6,8,11,71,72] about the mechanisms responsible for the very large values of Z_{eff} of some molecules. Gribakin [9] has expressed the view that values of Z_{eff} larger than a 1000 are not possible in a simple binary collision and that Feshbach resonances associated with vibrationally excited states need to be invoked. The present analysis tends to support at least the first aspect of this idea. The alternate view advanced by Laricchia and Wilkin [71] was that the large Z_{eff} were the consequence of exceptionally strong electron-positron correlations, in particular, very large rates for pick-off annihilation. However, their analysis has been severely criticized since there is almost no evidence to support their hypothesis [7,8,72].

VI. CONCLUSION AND OUTLOOK

Model-potential calculations have been performed for positron scattering from a number of atomic gases. There is nothing at all startling about the calculations of the elastic cross sections. In this respect, the calculation could be summarized as "just another calculation." However, the present work shows very clearly the strong connection between the annihilation and elastic cross sections that is implicit in the theory of Gribakin [8]. A calculation that correctly describes the energy dependence of the elastic cross section will largely reproduce the energy dependence of $Z_{eff}(k)$ even if the strong electron-positron correlations so important in an *ab initio* description of positron annihilation are omitted from the calculation. A single energy-independent scaling factor G seems to account for most of dynamical effects (i.e., strong electron-positron correlations) that lead to an enhanced Z_{eff}. These ideas have been exploited to determine estimates of the scattering length for Ar, Kr, and Xe.

The current model is not *ab initio* since the enhancement factor needs to be fixed by factors that are not contained within the theory. Further progress requires the development of methods to compute the enhancement factor from first principles. Dzuba *et al.* have discussed a number of ways to determine the enhancement factor [9]. However, their calculations are best described as estimates since they really did not aim to get precise numerical values for G. Enhancement factors derived from fits to electron-gas calculations are also widely used in the interpretation of positron-annihilation experiments in condensed-matter physics [73,74].

One new set of quantitative results are the estimates of Z_{eff} for a number of metal vapors. In contradiction to speculations based upon semiempirical formulas, the present calculations predict the threshold Z_{eff} for Be, Mg, and Cu to be of order 100. However, these are not the best metals for experimental work. Beryllium has a very high melting temperature while the low ionization potentials for Mg and Cu mean that Ps formation via collisions with the high-energy tail of the positron-energy distribution could interfere with any attempt to measure Z_{eff}. The group IIB metal vapors such as Zn and Cd with their higher ionization potentials and lower melting points would be much better candidates for experimental work. Using Be and Mg as a guide suggests that the threshold Z_{eff} for Zn and Cd should be 50–100. Better estimates of Z_{eff} for Zn and Cd will be made as soon as converged calculations of the positron binding energy and lifetimes of e^+Zn and e^+Cd become available.

[1] D. A. L. Paul and L. Saint-Pierre, Phys. Rev. Lett. **11**, 493 (1963).

[2] G. R. Heyland, M. Charlton, T. C. Griffith, and G. L. Wright, Can. J. Phys. **60**, 503 (1982).

[3] C. M. Surko, A. Passner, M. Leventhal, and F. J. Wysocki, Phys. Rev. Lett. **61**, 1831 (1988).

[4] I. Iwata, R. G. Greaves, T. J. Murphy, M. D. Tinkle, and C. M. Surko, Phys. Rev. A **51**, 473 (1995).

[5] Jun Xu, L. D. Hulett, T. A. Lewis, D. L. Donohue, S. A. McLuckey, and O. H. Crawford, Phys. Rev. A **49**, R3151 (1994).

[6] I. Iwata, G. F. Gribakin, R. G. Greaves, C. Kurz, and C. M. Surko, Phys. Rev. A **61**, 022719 (2000).

[7] G. G. Ryzhikh and J. Mitroy, J. Phys. B **32**, 2229 (2000).

[8] G. F. Gribakin, Phys. Rev. A **61**, 022720 (2000).

[9] V. A. Dzuba, V. V. Flambaum, G. F. Gribakin, and W. A. King, J. Phys. B **29**, 3151 (1996).

[10] V. A. Dzuba, V. V. Flambaum, W. A. King, B. M. Miller, and O. P. Sushkov, Phys. Scr., T **46**, 248 (1993).

[11] C. R. C. de Carvalho, M. T. D. N. Varella, M. A. P. Lima, E. P. da Silva, and J. S. E. Germano, Nucl. Instrum. Methods Phys. Res. B **171**, 33 (2000).

[12] E. P. da Silva, J. S. E. Germano, and M. A. P. Lima, Phys. Rev. A **49**, R1527 (1994).

[13] A. A. Giantuco and T. Mukherjee, Nucl. Instrum. Methods Phys. Res. B **171**, 17 (2000).

[14] P. A. Fraser, Adv. At. Mol. Phys. **4**, 63 (1968).

[15] R. P. McEachran, D. L. Morgan, A. G. Ryman, and A. D. Stauffer, J. Phys. B **10**, 663 (1977).

[16] G. G. Ryzhikh and J. Mitroy, J. Phys. B **32**, 4051 (1999).

[17] D. M. Schrader, Phys. Rev. A **1**, 1070 (1970).

[18] G. K. Ivanov, Dokl. Akad. Nauk SSSR **291**, 622 (1986) [Dokl. Phys. Chem. **291**, 1048 (1986)].

[19] S. W. Chiu and D. M. Schrader, Phys. Rev. A **33**, 2339 (1986).

[20] H. Nakinashi and D. M. Schrader, Phys. Rev. A **34**, 1823 (1986).

[21] R. Szmytkowski, Acta Phys. Pol. A **86**, 309 (1994).

[22] F. A. Gianturco and D. De Fazio, Phys. Rev. A **50**, 4819 (1994).

[23] J. E. Sienkiewicz and W. E. Baylis, Phys. Rev. A **40**, 3662 (1989).

[24] D. R. Reid and J. M. Wadehra, Phys. Rev. A **50**, 4859 (1994).

[25] L. T. Sinfailam, J. Phys. B **15**, 143 (1982).

[26] M. W. J. Bromley, J. Mitroy, and G. G. Ryzhikh, J. Phys. B **31**, 4449 (1998).

[27] T. M. Miller and B. Bederson, Adv. At. Mol. Phys. **13**, 1 (1984).

[28] W. Muller, J. Flesch, and W. Meyer, J. Chem. Phys. **80**, 3297 (1984).

[29] E. A. Reinsch and W. Muller, Phys. Rev. A **14**, 915 (1976).

[30] J. Mitroy, Aust. J. Phys. **48**, 645 (1995); **48**, 893 (1995).

[31] A. K. Bhatia, A. Temkin, R. J. Drachman, and H. Eiserike, Phys. Rev. A **3**, 1328 (1971).

[32] A. K. Bhatia, A. Temkim, and H. Eiserike, Phys. Rev. A **9**, 219 (1974).

[33] A. K. Bhatia, R. J. Drachman, and A. Temkin, Phys. Rev. A **9**, 223 (1974).

[34] A. K. Bhatia, R. J. Drachman, and A. Temkin, Phys. Rev. A **16**, 1719 (1977).

[35] P. Van Reeth and J. W. Humberston, J. Phys. B **32**, 3651 (1999).

[36] P. Van Reeth and J. W. Humberston, K. J. Iwata, R. J. Greaves, and C. M. Surko, J. Phys. B **29**, L465 (1996).

[37] R. P. McEachran, A. G. Ryman, and A. D. Stauffer, J. Phys. B **11**, 551 (1978).

[38] R. P. McEachran, A. G. Ryman, and A. D. Stauffer, J. Phys. B **12**, 1031 (1979).

[39] R. P. McEachran, A. D. Stauffer, and L. E. M. Campbell, J. Phys. B **13**, 1281 (1980).

[40] M. Charlton, Rep. Prog. Phys. **48**, 737 (1985).

[41] W. Kauppila and T. S. Stein, Can. J. Phys. **60**, 471 (1982).

[42] W. Kauppila and T. S. Stein, Adv. At. Mol. Phys. **26**, 1 (1990).

[43] I. Bray and A. T. Stelbovics, Phys. Rev. A **48**, 4787 (1993).

[44] J. Mitroy and G. G. Ryzhikh, J. Phys. B **32**, 2831 (1999).

[45] V. A. Dzuba, V. V. Flambaum, G. F. Gribakin, and C. Harabati, Phys. Rev. A **60**, 3641 (1999).

[46] M. W. J. Bromley, J. Mitroy, and G. G. Ryzhikh, Nucl. Instrum. Methods Phys. Res. B **171**, 47 (2000).

[47] T. J. Murphy and C. M. Surko, J. Phys. B **23**, L727 (1990).

[48] P. G. Coleman, T. C. Griffith, G. R. Heyland, and T. L. Killeen, J. Phys. B **8**, 1734 (1975).

[49] G. L. Wright, M. Charlton, T. C. Griffith, and G. R. Heyland, J. Phys. B **18**, 4327 (1985).

[50] J. Mitroy and G. G. Ryzhikh, J. Phys. B **34**, 2001 (2001).

[51] G. G. Ryzhikh and J. Mitroy, J. Phys. B **31**, 4459 (1998). The actual numbers given in Table I are slightly different as the model Hamiltonian and wave function for e^+Cu have been refined since publication.

[52] G. G. Ryzhikh, J. Mitroy, and K. Varga, J. Phys. B **31**, 3965 (1998).

[53] G. G. Ryzhikh and J. Mitroy, J. Phys. B **31**, 5013 (1998).

[54] J. Mitroy, M. W. J. Bromley, and G. G. Ryzhikh, J. Phys. B **32**, 2203 (1999).

[55] K. Iwata, G. F. Gribakin, R. G. Greaves, and C. M. Surko, Phys. Rev. Lett. **79**, 39 (1997).

[56] I. P. Grant, Adv. Phys. **19**, 747 (1970).

[57] J. P. D. Cook, J. Mitroy, and E. Weigold, Phys. Rev. Lett. **52**, 1116 (1984).

[58] P. G. Coleman, S. Rayner, F. M. Jacobsen, M. Charlton, and R. N. West, J. Phys. B **27**, 981 (1994).

[59] S. J. Ward and J. H. Macek, Phys. Rev. A **62**, 052715 (2000).

[60] A. Jain and D. G. Thompson, J. Phys. B **16**, 1113 (1983).

[61] L. Landau and E. M. Liftshitz, *Quantum Mechanics* (Pergamon, Oxford, 1965).

[62] Although the analysis in Sec. IV D is done in terms of a pole in the S matrix, it is noted that all the formulas could also be derived from an effective-range expansion of the cotangent of the phase shift. The S-matrix analysis was chosen since this is more keeping in theme with earlier work in the field.

[63] V. I. Goldanskii and Y. S. Sayasov, Phys. Lett. **13**, 300 (1964).

[64] V. I. Goldanskii and Y. S. Sayasov, Zh. Eksp. Teor. Fiz. **47**, 1995 (1964) [Sov. Phys. JETP **20**, 1339 (1965)].

[65] C. Kurz, R. G. Greaves, and C. M. Surko, Phys. Rev. Lett. **61**, 2929 (1996).

[66] C. M. Surko (private communication).

[67] T. J. Murphy and C. M. Surko, Phys. Rev. Lett. **67**, 2954 (1991).

[68] C. M. Surko, R. G. Greaves, K. Iwata, and S. J. Gilbert, Nucl. Instrum. Methods Phys. Res. B **171**, 2 (2000).

[69] J. Mitroy, J. Phys. B **33**, 5307 (2000).

[70] M. A. P. Lima (private communication).

[71] G. Laricchia and C. Wilkins, Phys. Rev. Lett. **79**, 2241 (1997).

[72] J. Mitroy and G. G. Ryzhikh, Phys. Rev. Lett. **83**, 3570 (1999).

[73] B. Barbiellini, M. Hakala, M. J. Puska, R. M. Nieminen, and A. A. Manual, Phys. Rev. B **56**, 7136 (1996).

[74] G. Kontrym-Sznajd and A. Rubaszek, Phys. Rev. B **47**, 6950 (1993).